COLOR MATCHING FUNCTIONS FOR A PERCEPTUALLY UNIFORM RGB SPACE

Joanna Marguier and Sabine Süsstrunk

School of Computer and Communication Sciences (IC)

Ecole Polytechnique Fédérale de Lausanne (EPFL)

Lausanne, Switzerland

ABSTRACT

We present methods to estimate perceptual uniformity of color spaces and to derive a perceptually uniform RGB space using geometrical criteria defined in a logarithmic opponent color representation.

1. INTRODUCTION

RGB color spaces play an important role in imaging: images captured with most digital cameras and displayed on CRT or LCD monitors are encoded in RGB. When we edit an image and modify one of its color attributes, such as lightness, we do not want to see shifts of the other attributes, hue and saturation. Similarly, simple non linear operations, like contrast modification, should only induce perceptually relevant changes. Both can be achieved by using a perceptually uniform encoding.

Opponent color spaces, like CIELAB 1976, are used to evaluate color difference in color imaging applications. CIELAB is based on the CIE 1931 XYZ color matching functions (CMFs). The non-linear relations for L, a and b values are an attempt to model the non-linear and opponent response of the human visual system, and to derive a color space representation where perceptually relevant color differences can be calculated with Euclidian distance.

In imaging applications, simpler transforms using opponent color representation, such as YCrCb or HSV are successfully used. It seems that for many applications, an approximation of a perceptual color space is sufficient for engineering tasks.

In this paper, we present methods to derive a perceptually uniform RBG color space where color differences can be measured as Euclidian distances. Our optimization criteria are not based on any knowledge of the human visual system but rely only on geometrical criteria defining space uniformity. Our transform has the form of a colorimetric color space [1]: a linear transform is applied to XYZ tristimulus values, followed by a non linear color component transfer function. Those values are then represented in an opponent space, where color attributes can easily be defined and distances measured. The optimization criteria are the straightness of hue lines, uniformity of hue angles and chroma.

The resulting RGB color spaces have better perceptual uniformity than both sRGB [2] and ROMM [3] transforms, but do not have a suitable gamut to be used as color image encodings. However, they also have similar perceptual uniformity than IPT [4] and CIELAB opponent color spaces.

2. EXPERIMENT

Our experiment is an extension of the work of Finlayson and Süsstrunk [5]. Using hue-constant psychophysical data by Hung and Berns [6], they derived hue-constant RGB color matching functions. They tested a large set of possible linear transforms from the CIE XYZ 1931 color matching functions. Each transform was applied to Hung and Berns hue-constant XYZ values. The obtained RGB values were then represented in a logarithmic opponent color space. The straightness of each hue line was estimated by singular values decomposition (SVD) line fitting.

Brightness and Gamma Invariant Hue

Hue can be defined independently from gamma and brightness [5, 7]. RGB vectors are encoded as:

$$\begin{bmatrix} R \\ G \\ B \end{bmatrix} = \begin{bmatrix} \alpha R_{lin}^{\gamma} \\ \alpha G_{lin}^{\gamma} \\ \alpha B_{lin}^{\gamma} \end{bmatrix} \quad (1),$$

where γ compensates for the system's non-linearity and α compensates for illuminance. Applying a logarithm removes γ from the exponent When taking the differences, followed by the ratio, both γ and α cancel out:

$$h_{hue} = \tan^{-1}\frac{\log(R_{lin}) - \log(G_{lin})}{\log(R_{lin}) + \log(G_{lin}) - 2\log(B_{lin})} \quad (2)$$

Spherical sampling

We use a spherical sampling technique to find the optimal transform [8]. Each triplet of points on the unit sphere represents one possible 3x3 transform from XYZ to RGB (**T**). By testing all triplets, we can test transforms exhaustively. For computational reasons though, we initially limited the tested transforms to those located within 45° of the sRGB transform [2]. We had to slightly extend the sampling points area to reach a minimum.

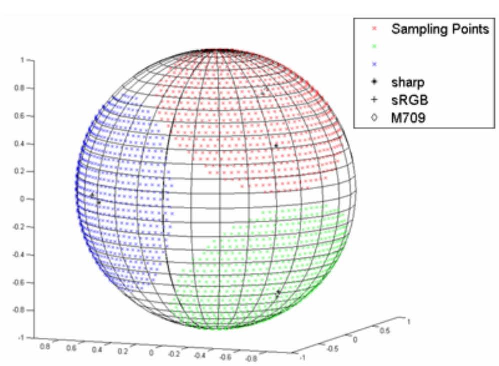

Figure 1: Sampling points

Data

We first use Munsell renotation data [9], Simulations were run on the "real" XYZ tristimulus values, i.e. representing colors lying inside the MacAdam limits [10]. It represents a dataset of 390 values distributed in 40 hue angles, defined under illuminant C. We used the Sharp chromatic adaptation transform [11] to calculate corresponding colors under D65. Hung and Berns data [12] were also used for comparison.

Logarithmic Opponent Color Calculation

XYZ values are converted into linear RGB by applying the (3x3) transform **T** found through the spherical sampling technique. We ignore negative RGB values instead of offsetting or compressing them. The number of positive RGB values *N* may thus vary for each transform. We take into account only transforms giving at least 67% of positive values.

The log opponent color matrix **O** (*N*x2) is calculated from the (*N*x3) RGB matrix according to

$$\mathrm{O} = [\log(R_{lin}) - \log(G_{lin}), \log(R_{lin}) + \log(G_{lin}) - 2\log(B_{lin})] \quad (3)$$

Singular values decomposition line fitting

Hue constant data should lie on a line in the log opponent hue representation. Hue lines are evaluated using a singular values decomposition method. The deviation of hue values from the fitted line gives an estimation of hue constancy. We add the constraint that the line should pass through the origin. This is done by mirroring all opponent colors values resulting in a (2*N*x2) matrix $\mathbf{H} = [\mathbf{O}; \mathbf{-O}]$.

Prior to line fitting, the components are decorrelated using a whitening transform. This transform is based on the eigenvalue decomposition of the covariance matrix $(\mathbf{H}^{\mathrm{T}}\mathbf{H})$ of $\mathbf{H}$.

$$\mathbf{H}^{\mathrm{T}}\mathbf{H} = \mathbf{E}\mathbf{\Lambda}\mathbf{E}^{\mathrm{T}} \quad (4)$$

$\mathbf{H}$ then becomes

$$\tilde{\mathbf{H}} = \mathbf{H}(\mathbf{E}\mathbf{\Lambda}^{1/2})^{T} \quad (5)$$

The matrix $\tilde{\mathbf{H}}$ is then separated into 40 matrices $\tilde{\mathbf{H}}_{\mathbf{n}}$, each corresponding to a hue line and containing the log opponent RGB values and their mirrored values.

The singular value decomposition is

$$\tilde{\mathbf{H}}_{\mathrm{n}} = \mathbf{U}_{\mathrm{n}}\mathbf{D}_{\mathrm{n}}\mathbf{V}_{\mathrm{n}}^{\mathrm{T}} \quad (6)$$

Where $\mathbf{U}_{\mathrm{n}}$ and $\mathbf{V}_{\mathrm{n}}$ contain singular vectors and $\mathbf{D}_{\mathrm{n}}$ is a diagonal matrix of singular values,

$$\mathrm{D}_{\mathrm{n}} = \begin{pmatrix} \sigma_1(n) & 0 \\ 0 & \sigma_2(n) \end{pmatrix} \quad (7)$$

The second singular value σ_2 is the residual error, i.e., the distance between the points and the fitted line.

For one given transform, the residual error is the mean error over all 40 hues.

$$\varepsilon = \frac{1}{40}\sum_{n=1}^{40}\sigma_2(n) \quad (8)$$

The residual error also varies with the square root of the number of fitted points, i.e.

$$\sigma_2^{norm}(n) = \frac{1}{\sqrt{N}}\sigma_2(n)\ , \quad (9)$$

where *N* is the number of positive values.

Using equations (8) and (9), the residual error is given by

$$\varepsilon^{norm} = \frac{1}{40}\frac{1}{\sqrt{N}}\sum_{n=1}^{40}\sigma_2(n) \quad (10)$$

Finally, each set of opponent RGB values were normalized prior to line fitting using their extreme values so that the range of values does not have an influence on the residual error. For each hue line separately

$$x' = \frac{x}{x_{\max} - x_{\min}} \text{ and } y' = \frac{y}{y_{\max} - y_{\min}}\ , \quad (11)$$

where *x* and *y* are the red-green and yellow-blue opponent coordinates, respectively.

Optimization criteria

Hue constancy

Optimizing for hue constancy alone will not result in a perceptually uniform space, it only gives a measure of hue constancy for increasing chroma. Hence we introduced other criteria on the geometrical representation.

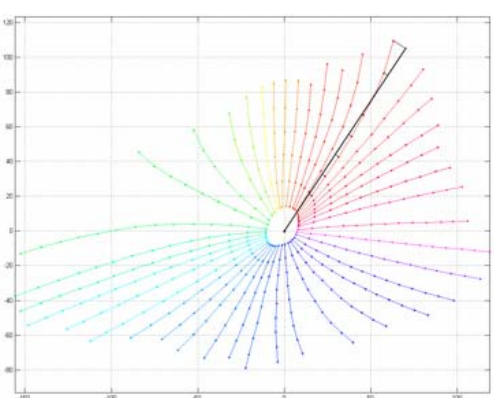

Figure 2: line fitting
x-axis: log(R)-log(G), y-axis: log(R)+log(G)-2log(B)

Hue angle uniformity

The second criterion is the uniformity of hue angles. Using Munsell renotation data, the angle between each pair of adjacent hue lines should be 360°/40 hues = 9° (see Figure 3). SVD line fitting returns unit vectors normal to the line. The angles between two lines can thus be computed using:

$$\alpha_i = \cos^{-1}(\vec{n_i} \circ \overrightarrow{n_{i+1}}) \quad (12)$$

The variance of the 40 angles around 9° is then computed. A low variance indicates good angle uniformity.

The variance is given by:

$$\sigma_h = \frac{1}{40}\sum_{i=1}^{40}(\alpha_i - 9°)^2 \quad (13)$$

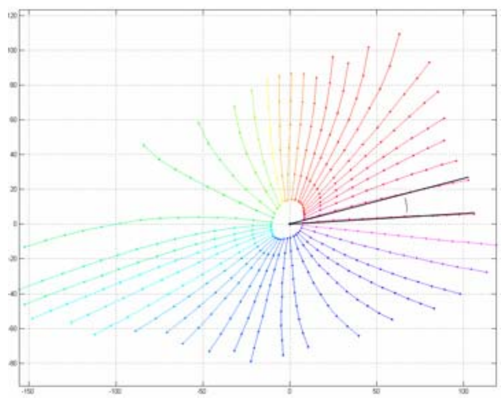

Figure 3: uniform hue angles
x-axis: log(R)-log(G), y-axis: log(R)+log(G)-2log(B)

Chroma uniformity

The third criterion uses color distances on each hue line. Supposing the distance between every two pairs of XYZ Munsell values to be perceptually equal, we compute the distances between each pairs of adjacent points on one hue line and store them in a vector **d**:

$$\mathrm{d}(i) = \sqrt{(x(i+1) - x(i))^2 + (y(i+1) - y(i))^2} \quad (14)$$

Where *x* and *y* are the red-green and yellow-blue opponent coordinates, respectively and the index *i* runs over the chroma.

The vector **d** is computed for every hue line and the 40 vectors are then concatenated into a 350x1 vector **D**. The variance is computed as:

$$\sigma_D = \frac{1}{350}\sum_{i=1}^{350}(\mathrm{D}(i) - \overline{\mathrm{D}})^2 \quad (15)$$

A low variance on the intervals lengths is an indicator of good chroma uniformity.

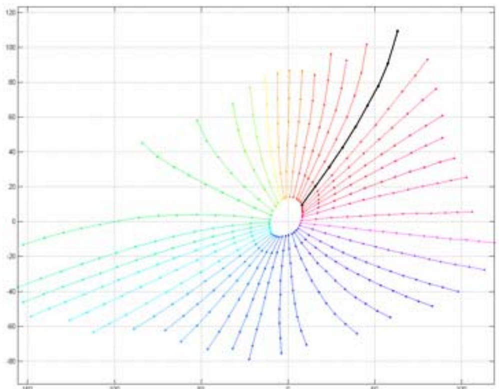

Figure 4: intervals
x-axis : log(R)-log(G), y-axis: log(R)+log(G)-2log(B)

The eccentricity of chroma circles is also a condition for good space uniformity. Uniform hue angles plus uniform color differences imply that chroma circle eccentricity is close to zero.

Note that the whitening transform was only used to estimate hue constancy, as it would have falsely influenced the other criteria. The variances on color differences and hue angle uniformity were computed using non normalized logarithm opponent color values.

3.RESULTS

We tested over 300 millions different transforms. We only kept the transforms having line fitting residual errors, angles and intervals variances comparable to IPT and CIELAB's. It represents a total of 660 transforms.

In this section, we present the results for each individual optimization criterion and the overall solution. The results are then compared with CIE Lab and IPT transforms.

In the last section, we present results using the same criteria but performed on Hung and Berns hue constant dataset.

Transform 1: Best hue constancy

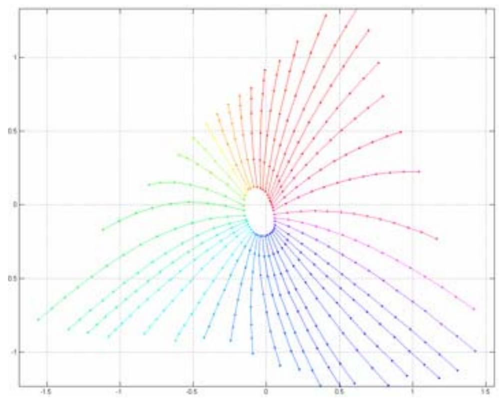

Figure 5: best hue constancy
x-axis: log(R)-log(G), y-axis: log(R)+log(G)-2log(B)

Transform 2: Best hue angles uniformity

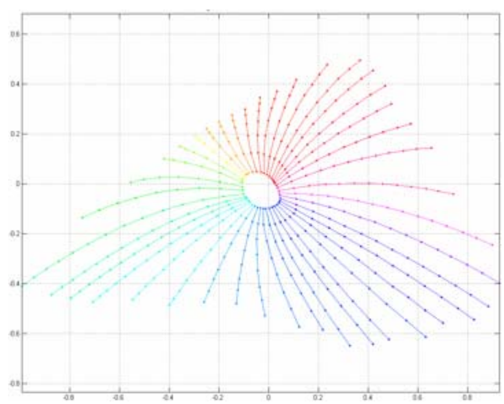

Figure 6: best hue angle uniformity
x-axis: log(R)-log(G), y-axis: log(R)+log(G)-2log(B)

Transform 3: Best chroma uniformity

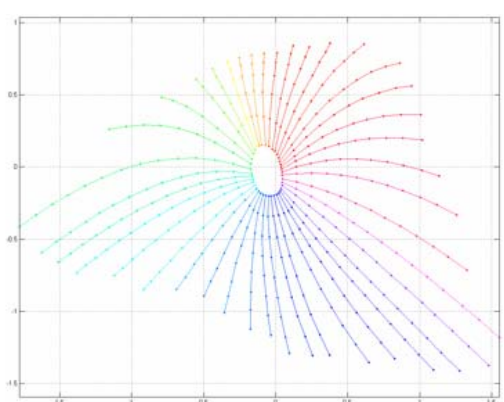

Figure 7: lowest intervals length variance
x-axis: log(R)-log(G), y-axis: log(R)+log(G)-2log(B)

Combining all criteria

The three space uniformity indicators, angle variance, interval lengths variance and line fitting residual error, represented in a three dimensional space define a function. Its minimum is the point located at the shortest distance from the origin. The corresponding transform defines the overall best transform. This transform is the one having the lowest interval lengths variance, i.e. it is also transform 3.

Corresponding sensors

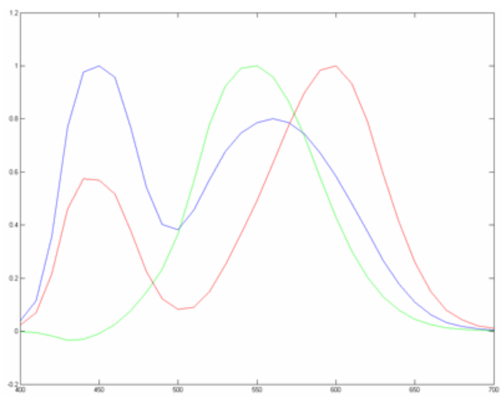

Figure 8: best transform's corresponding sensors

Comparison with CIELAB and IPT

Table 1 shows the space uniformity indicators for CIELAB, IPT, sRGB and ROMM transforms as well as for the three transforms obtained through our optimization.

	ε residual err	σ angles	σ intervals
IPT	0.0147	0.0045	0.0836
CIELAB	0.0123	0.0074	0.0498
sRGB	0.0267	0.0242	0.4551
ROMM	0.0204	0.0257	0.4743
transform 1	**0.0122**	0.0056	0.0551
transform 2	0.0156	**0.0021**	0.0560
transform 3	0.0159	0.0041	**0.0400**

Table 1: uniformity indicators for several transforms using Munsell dataset

Dependency on the data set

We performed the same optimization using the same criteria on Hung and Berns hue constant data set.

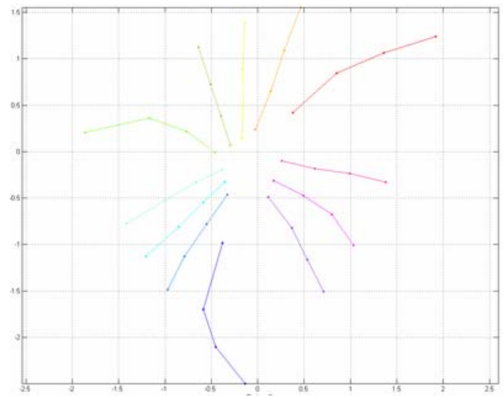

Figure 9: overall minimum using Hung and Berns dataset
x-axis: log(R)-log(G), y-axis: log(R)+log(G)-2log(B)

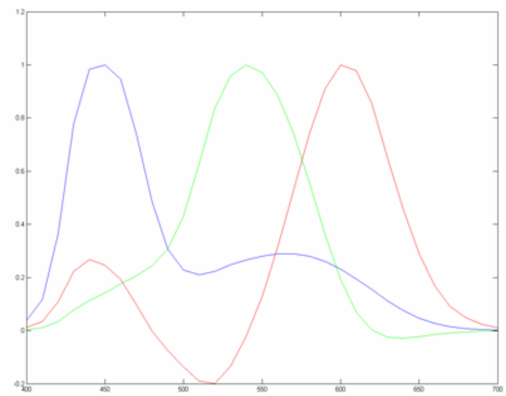

Figure 10: corresponding sensors

Corresponding gamuts

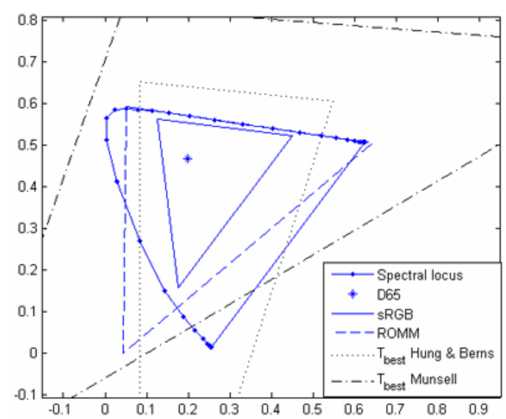

Figure 11: Lu'v' diagram and gamuts

4. CONCLUSION

We do not obtain definitive results, the optimal transform depends strongly on the dataset used to perform the optimization.

Considering the angles, intervals lengths and hue constancy computed for both CIELAB and IPT, CIELAB shows better hue constancy than IPT. On the other hand, when we compute the same indicators for Hung and Berns hue constant data, IPT gives much better results. The quality of the result depends on the perceptual relevancy of the dataset.

We do not obtain transforms that have all space uniformity indicators – hue constancy, hue angle uniformity and interval lengths uniformity – lower that IPT and CIELAB's, but we obtain a much better space uniformity that sRGB or ROMM RGB.

The gamut extent of the resulting transforms has too much values lying outside the spectral locus to be used as a color encoding. However, this representation can still be used to estimate color differences using a Euclidian metric.

The mathematical tools presented here are applicable for evaluation of color space uniformity and further optimizations taking more criteria into account – like the gamut extent – can be carried out.

The logarithmic opponent color definition we are using here [5, 7] might not be appropriate for space uniformity evaluation, the use of the power function instead may give better results.

REFERENCES

[1] ISO 22028-1:2004, Photography and graphic technology, Extended colour encodings for digital image storage, manipulation and interchange, Part 1: Architecture and requirements.

[2] IEC 61966-2-1: 1999. Multimedia systems and equipment, Colour measurement and management, Part 2-1: Colour management, Default RGB colour space, sRGB.

[3] K.E. Spaulding, G.J. Woolfe, and E.J. Giorgianni, "Optimized extended gamut color encoding for scene-referred and output referred image states," J. Imaging Science and Technology, 45(5), pp. 418-426, 2001.

[4] F. Ebner and M.D. Fairchild, "Development and Testing of a Color Space (IPT) with Improved Hue Uniformity," Proc. IS&T/SID 6th Color Imaging Conference, pp.8-13, 1998.

[5] G.D. Finlayson and S. Süsstrunk, "Optimization for Hue Constant RGB sensors," Proc. IS&T/SID 10th Color Imaging Conference, 2002.

[6] P. Hung and R. Berns, "Determination of constant hue loci for a CRT gamut and their prediction using color appearance spaces," Color Research and Applications, 20, pp. 285-295, 1995.

[7] G.D. Finlayson and G. Schaefer, "Hue that is invariant to brightness and gamma," Proc. British Machine Vision Conference, 2000.

[8] G.D. Finlayson and S. Süsstrunk, "Spherical sampling and color transformations," Proc. IS&T/SID 9th Color Imaging Conference, 2001.

[9] Munsell renotation data, RIT Munsell Color Science Laboratory.

[10] Newhall, Nickerson, and Judd, Final report of the OSA subcomittee on the spacing of the Munsell colours, Journal of the Optical Society of America, A, 33:385–418, 1943.

[11] S. Süsstrunk, J. Holm and G.D. Finlayson, "Chromatic adaptation performance of different RGB sensors," Proc. IS&T/SPIE Electronic Imaging 2001: Color Imaging, Vol. 4300, pp. 172-183, 2001.

[12] P. Hung and R. Berns, "Determination of constant hue loci for a CRT gamut and their prediction using color appearance spaces," Color Research and Applications, 20, pp. 285-295, 1995.

Authors:
Joanna Marguier
School of Computer and Communication Sciences
Ecole Polytechnique Fédérale de Lausanne
Lausanne, Switzerland

Phone: (+41 21) 693 12 72
Fax: (+41 21) 693 43 12
e-mail: Joanna.Marguier@epfl.ch